Frontiers of Physics
https://doi.org/10.1007/s11467-021-1149-7
Front. Phys.
17(5), 53503 (2022)

RESEARCH ARTICLE

Vector valley Hall edge solitons in the photonic lattice with type-II Dirac cones

Yiqing Tian[1], Yiqi Zhang[1,†], Yongdong Li[1], Milivoj R. Belić[2]

[1] *Key Laboratory for Physical Electronics and Devices of the Ministry of Education & Shaanxi Key Lab of Information Photonic Technique, School of Electronic and Information Engineering, Xi'an Jiaotong University, Xi'an 710049, China*
[2] *Science Program, Texas A&M University at Qatar, P.O. Box 23874 Doha, Qatar*
Corresponding author. E-mail: [†] *zhangyiqi@xjtu.edu.cn*
Received December 11, 2021; accepted January 21, 2022

Topological edge solitons represent a significant research topic in the nonlinear topological photonics. They maintain their profiles during propagation, due to the joint action of lattice potential and nonlinearity, and at the same time are immune to defects or disorders, thanks to the topological protection. In the past few years topological edge solitons were reported in systems composed of helical waveguide arrays, in which the time-reversal symmetry is effectively broken. Very recently, topological valley Hall edge solitons have been demonstrated in straight waveguide arrays with the time-reversal symmetry preserved. However, these were scalar solitary structures. Here, for the first time, we report vector valley Hall edge solitons in straight waveguide arrays arranged according to the photonic lattice with innate type-II Dirac cones, which is different from the traditional photonic lattices with type-I Dirac cones such as honeycomb lattice. This comes about because the valley Hall edge state can possess both negative and positive dispersions, which allows the mixing of two different edge states into a vector soliton. Our results not only provide a novel avenue for manipulating topological edge states in the nonlinear regime, but also enlighten relevant research based on the lattices with type-II Dirac cones.

Keywords valley Hall effect, topological edge soliton, photonic topological insulator

1 Introduction

Topological insulators originated in condensed matter physics [1, 2] but speedily moved into other branches of physics, such as mechanics [3, 4], acoustics [5, 6], optoelectronics [7, 8], atomics [9, 10], and photonics [11–18]. In fact, the whole field of "topological photonics" [19–27] has come into being recently and is becoming ever more significant, both in basic science and applications. After more than a decade in development, owing to unique advantages of the photonic platform in marrying lattice potentials and nonlinearity [28] and in fabricating non-Hermitian configurations [29, 30], topological photonics is fast claiming a prominent place among the new fields of nonlinear science.

Recent progress in the subject indeed demonstrates an increasingly important role that nonlinearity plays in optics and has inspired the emergence of novel phenomena in topological photonic systems. Typical examples include topological insulator lasers [31–40], nonlinearity-induced topological transitions [41], bistability [42, 43], and topological edge solitons. Owing to their topological nature, these solitons represent localized bound states that move with constant speed along the edges of the sample. On one hand, they are immune to the influence of defects or disorders when propagating along the boundary, because of the topological protection, and on the other hand, they maintain their envelopes due to the nonlinear self-action.

In the photonic Floquet topological insulators, the time-reversal symmetry, which is broken by the artificial magnetic field due to the helicity of waveguide arrays, topologically closed currents in the bulk were first reported in theory [44] and then in experiment [45]. Originating from the linear edge states, the topological edge solitons in Floquet systems were first investigated in depth in discrete [46–48] and then in continuous [49–55] models. In polariton-based topological insulators, in which time-reversal symmetry is broken by the authentic magnetic field due to the spin-orbit coupling, the topological edge solitons were also reported in theory [56–59]. In addition to the aforementioned topological edge solitons, the Dirac solitons [60], Bragg solitons [61], and valley Hall edge solitons [62–64] have also been brought to close scrutiny in various topological systems. However, experimental observation of topological edge solitons is still an open problem, since thus far only their non-topological counterparts were experimentally realized [65], to the best of our knowledge.

It is worth mentioning that among various topological

* This article can also be found at http://journal.hep.com.cn/fop/EN/10.1007/s11467-021-1149-7.

edge solitons, the vector topological edge solitons have received insufficient attention, except for those in photonic Floquet insulators [52, 53]. The reason is rather obvious — the difficulty in observing such complex structures. A vector soliton generally contains more than one component that closely couple together. Therefore, in comparison with scalar solitons, vector solitons are not only more challenging in realization but also more inspiring for potential applications.

The purpose of this paper is to demonstrate vector topological edge solitons resulting from the valley Hall effect [66], which are important as the next building blocks to scalar solitons, but were not explored before. As the building platform we choose the photonic lattice with innate type-II Dirac cones [67]. The overriding reason for choosing such a lattice is that the dispersion of the valley Hall edge state contains two distinct regimes, which could support bright and dark solitons simultaneously. This property is necessary but not sufficient for the construction of vector solitons, and moreover it is seemingly impossible to realize in the honeycomb lattice [63, 64]. Therefore, the honeycomb lattice [68] is not convenient for the investigation of vector valley Hall edge solitons at the current level of cognition. In addition, in the lattice with type-II Dirac cones lacking C_3 symmetry [69], one cannot design a domain wall with sharp corners for checking the topological protection of the valley Hall edge solitons. As a result, one has to find a substitution — the large-scale defect capable of demonstrating the robustness of valley Hall edge solitons [62]. The next section introduces a model that accommodates all the necessary conditions.

2 The model

The propagation dynamics of a light beam in a lattice is governed by the dimensionless Schrödinger-like equation with cubic focusing nonlinearity,

$$\mathrm{i}\frac{\partial\psi}{\partial z} = -\frac{1}{2}\left(\frac{\partial^2}{\partial x^2} + \frac{\partial^2}{\partial y^2}\right)\psi - \mathcal{R}(x,y)\psi - |\psi|^2\psi, \qquad (1)$$

in which the propagation distance z plays a role of time t. Here ψ is the complex envelope wave function and $\mathcal{R}$ is the lattice potential with type-II Dirac cones that is described by the function

$$\mathcal{R}(x,y) = -\sum_{n,m} p_{\mathrm{in}}\mathcal{Q}\left(x - x_n, y - y_m\right), \qquad (2)$$

where the individual Gaussian potential wells, described by $\mathcal{Q}(x,y) = \exp[-(x^2+y^2)/d^2]$ with $d = 0.5$, are placed at the nodes of the grid (x_n, y_m). This structure is periodic in the y direction: $\mathcal{R}(x,y) = \mathcal{R}(x, y+Y)$ with the period $Y = a$, where $a = 1.4$ is the lattice constant. To better discern the lattice, we label the three different sites in one unit cell as A, B and C, respectively, as shown in Fig. 1(c).

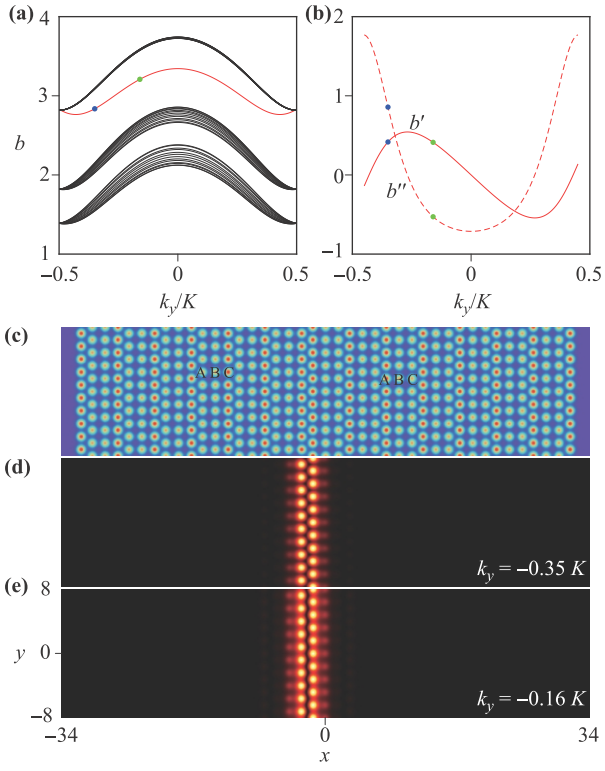

Fig. 1 **(a)** Band structure of the photonic lattice ribbon with a domain wall shown in (c). Black curves correspond to bulk states and the red curve is the topological edge state. **(b)** The first-order b' (solid curve) and the second-order b'' (dashed curve) derivative of the edge state. The values of the first-order derivative for the blue and green dots are ~ 0.42, while the second-order derivatives are ~ 0.86 and ~ -0.53, respectively. **(c)** Photonic lattice with a domain wall composited by two inversion-symmetry-broken lattices. **(d–e)** Profiles of selected topological edge states at $k_y = -0.35K$ and $k_y = -0.16K$, corresponding to the blue and green dots in (a, b).

The corresponding well depths are labeled as p_A, p_B and p_C. If $p_A = p_B = p_C = p_{\mathrm{in}}$, the inversion symmetry of the lattice is preserved, while if a detuning δ is introduced in one of them, the inversion symmetry is broken. We choose two arrays with broken inversion symmetry and combine them within a domain wall, as shown in Fig. 1(c). On the left-hand-side of the domain wall, $p_A = p_B = p_{\mathrm{in}} = 8$ and $p_C = p_{\mathrm{in}} + \delta = 10$, while on the right-hand-side of the domain wall, $p_B = p_C = p_{\mathrm{in}} = 8$ and $p_A = p_{\mathrm{in}} + \delta = 10$.

Assuming that waveguide arrays are prepared by using the femtosecond laser writing technique in fused silica [16, 41, 45, 70–72], the normalized parameters described above can be substituted by experimental values. Provided the laser radiation at the wavelength of 800 nm is used and the characteristic transverse scale is set to 10 μm that corresponds to dimensionless coordinates $x, y = 1$, the array constant turns out to be 14 μm, the waveguide width is 5 μm, and $p_{\mathrm{in}} = 8$ corresponds to the refractive index modulation depth of $\sim 8.8 \times 10^{-4}$. We believe

that the findings in the following text can be experimentally observed with the method and parameters mentioned above.

An assumption behind Eq. (1) is that the influence of nonlinearity is small. Therefore, one starts from the energy band structure of the lattice without the nonlinear term and builds the sought-for solutions from there. By inserting an ansatz $\psi(x,y,z) = \phi(x,y)\exp(\mathrm{i}bz)$ with $\phi(x,y) = u(x,y)\exp(\mathrm{i}k_y y)$ into Eq. (1), one obtains the following eigenvalue problem

$$bu = \frac{1}{2}\left(\frac{\partial^2}{\partial x^2} + \frac{\partial^2}{\partial y^2} + 2\mathrm{i}k_y\frac{\partial}{\partial y} - k_y^2\right)u + \mathcal{R}u, \tag{3}$$

where $u(x,y) = u(x,y+L)$ is the periodic Bloch wave function, $k_y \in [-K/2, K/2)$ is the Bloch momentum in the first Brillouin zone with $K = 2\pi/L$, and b is the propagation constant of the linear mode that is a function of k_y.

Based on the plane-wave expansion method, the band structure corresponding to the composite lattice is displayed in Fig. 1(a), in which there is one edge state in the top (first) band gap according to the bulk-edge correspondence principle [20], as indicated by the red curve. To seek for more intricate properties of these edge states, the first-order derivative $b' = \mathrm{d}b/\mathrm{d}k_y$ and the second-order derivative $b'' = \mathrm{d}^2b/\mathrm{d}k_y^2$ are explored, as shown in Fig. 1(b). As is well known, $-b'$ estimates the velocity of the edge state while b'' is responsible for the acceleration, that is, the dispersion of the wave. One finds that b'' is positive around the middle of the first Brillouin zone (BZ), and negative around the edge of the first BZ.

According to the condition for constructing bright and dark solitons, one may expect to find bright edge solitons based on the edge states around the middle of the first BZ and dark solitons around the edge of the BZ. Hence, we choose two valley Hall edge states in two different regimes, as shown in Fig. 1(a), and display their profiles in Figs. 1(d) and (e), with the Bloch momenta exhibited in the right-bottom corner of each panel. Clearly, edge states corresponding to the blue and green dots support dark and bright solitons, respectively. Since both signs of the first-order derivatives of the two selected edge states are positive with nearly equal values ~ 0.42, the two edge states as well as their bifurcated solitons will move along the same direction synchronously — the negative y axis — during propagation. In the following, all solitons considered here are based on the two edge states marked with blue and green dots. Based on these considerations, one can not only construct scalar solitons but also vector solitons.

To construct the vector solitons, we follow the approach utilized in the previous literature [52, 53] and consider bifurcation from the linear Bloch states. We are looking for the vector topological edge solitons, so we assume a solution in the form

$$\psi = A_\alpha(Y,z)\phi_\alpha\exp(\mathrm{i}b_\alpha z) + A_\beta(Y,z)\phi_\beta\exp(\mathrm{i}b_\beta z),$$

where $A_{\alpha,\beta}$ are the slowly-varying amplitudes and $Y = y - v_{\alpha,\beta}z$ is the coordinate in the frame of reference moving with velocity $v_{\alpha,\beta} = -b'_{\alpha,\beta}$ for both components. The evolution of the envelopes is then governed by the coupled nonlinear Schrödinger-like equations

$$\begin{aligned}
\mathrm{i}\frac{\partial A_\alpha}{\partial z} &= \frac{b''_\alpha}{2}\frac{\partial^2 A_\alpha}{\partial Y^2} - \left(\chi_\alpha|A_\alpha|^2 + 2\chi|A_\beta|^2\right)A_\alpha,\\
\mathrm{i}\frac{\partial A_\beta}{\partial z} &= \frac{b''_\beta}{2}\frac{\partial^2 A_\beta}{\partial Y^2} - \left(\chi_\beta|A_\beta|^2 + 2\chi|A_\alpha|^2\right)A_\beta,
\end{aligned} \tag{4}$$

where $\chi_\nu = \langle|\phi_\nu|^2, |\phi_\nu|^2\rangle$ and $\chi = \langle|\phi_\alpha|^2, |\phi_\beta|^2\rangle$. The inner product $\langle f, g\rangle := \int_S f^* g\mathrm{d}x\mathrm{d}y$ is performed over the entire array area S. Numerically, Eqs. (4) can be solved by using Newton method in the form $A_\nu(Y,z) = w_\nu(Y)\exp(\mathrm{i}b_\nu^{\mathrm{nl}}z)$ with $\nu = \alpha,\beta$, where b_ν^{nl} is the nonlinearity-induced phase shift, which should be sufficiently small to make sure that the profile $w_\nu(Y)$ is broad and fulfills the slowly-varying envelope requirements. When $\chi = 0$, the vector solitons reduce to the scalar solitons, with the analytical solutions given by

$$A_\nu = \sqrt{2\frac{b_\nu^{\mathrm{nl}}}{\chi_\nu}}\,\mathrm{sech}\left(\sqrt{-2\frac{b_\nu^{\mathrm{nl}}}{b''_\nu}}Y\right)\exp\left(-\mathrm{i}b_\nu^{\mathrm{nl}}z\right) \tag{5}$$

for bright solitons, and

$$A_\nu = \sqrt{\frac{b_\nu^{\mathrm{nl}}}{\chi_\nu}}\,\tanh\left(\sqrt{\frac{b_\nu^{\mathrm{nl}}}{b''_\nu}}Y\right)\exp\left(-\mathrm{i}b_\nu^{\mathrm{nl}}z\right) \tag{6}$$

for dark solitons.

3 Results and discussion

3.1 Envelopes of valley Hall edge solitons

To start with, we discuss the scalar soliton envelopes, based on the analytical solutions in Eqs. (5) and (6). In Figs. 2(a) and (b), we display the envelopes of the bright soliton and the dark soliton, with $b^{\mathrm{nl}} = 0.004$ and $b^{\mathrm{nl}} = 0.0016$, respectively. The bigger the value of b^{nl}, the narrower the width of the soliton.

Different from the scalar solutions, the envelopes of vector solutions must be calculated numerically again, by using Newton method. In Fig. 2(c), we show one example of the vector bright-dark soliton envelopes, with $b_\alpha^{\mathrm{nl}} = 0.004$ and $b_\beta^{\mathrm{nl}} = 0.0016$. While in Fig. 2(d), another type of vector soliton envelopes is exhibited, with $b_\alpha^{\mathrm{nl}} = 0.005$ and $b_\beta^{\mathrm{nl}} = 0.002$. Note that the envelope indicated by the black curve is neither a dark soliton nor a gray soliton, the phase

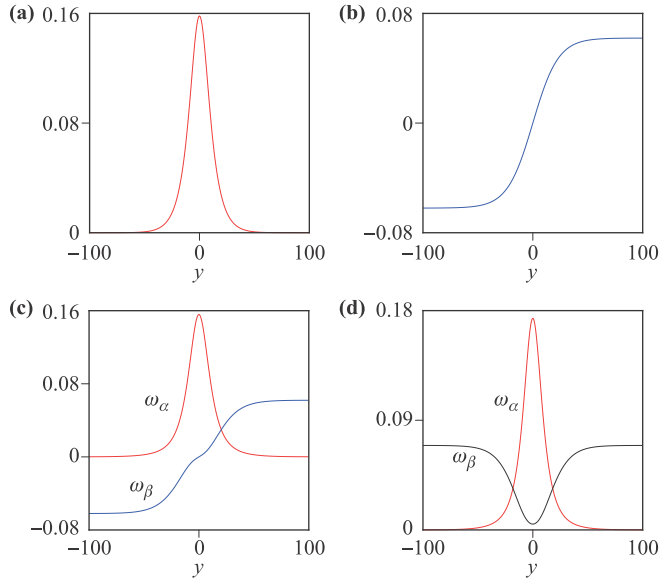

Fig. 2 **(a)** Envelope of the bright soliton with $b^{\rm nl} = 0.004$. **(b)** Envelope of the dark soliton with $b^{\rm nl} = 0.0016$. **(c)** Envelopes of the bright-dark vector soliton with $b_\alpha^{\rm nl} = 0.004$ and $b_\beta^{\rm nl} = 0.0016$. **(d)** Envelopes of the bright-anti-bright vector soliton with $b_\alpha^{\rm nl} = 0.005$ and $b_\beta^{\rm nl} = 0.002$.

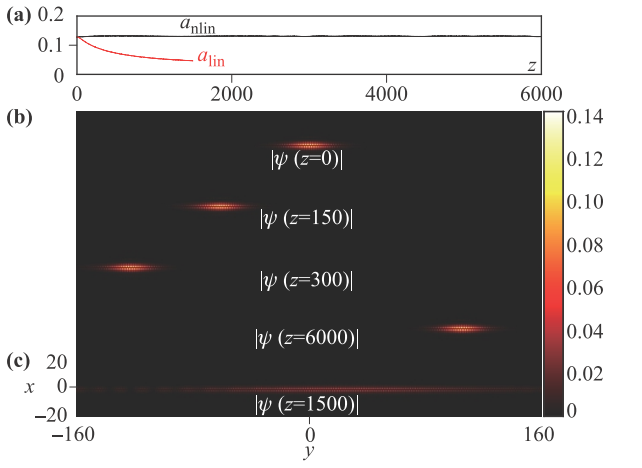

Fig. 4 Moving bright topological valley Hall edge soliton with $b^{\rm nl} = 0.004$. **(a)** Peak amplitudes of the soliton input during long propagation. Black curve shows the nonlinear propagation of $a_{\rm nlin}$ which does not decay after a long distance, while the red one represents the linear propagation of $a_{\rm lin}$ which decays quickly. **(b)** Profiles of the bright soliton at selected propagation distances. **(c)** Profile of the same input as in (b) after a linear propagation of $z = 1500$.

of which possesses a π shift across $y = 0$. Unlike dark, the gray soliton does not reach zero at $y = 0$. This is a completely new component that is not reported before in topological photonics, to the best of our knowledge. Here, we call this component the *anti-bright* soliton.

Similar to the scalar solitons, the vector solitons also depend on $b_{\alpha,\beta}^{\rm nl}$. To quantify this dependence, we record the peak amplitude of the bright component a_α and the background of the dark (or anti-bright) component a_β, by fixing $b_\alpha^{\rm nl} = 0.005$ and scanning the value of $b_\beta^{\rm nl}$. The results are shown in Fig. 3. When $b_\beta^{\rm nl} = 0$, the vector case reduces to the scalar case, and the dark (anti-bright) component disappears. With increasing $b_\beta^{\rm nl}$, the dark (anti-bright) component emerges gradually and the background enlarges synchronously. At the same time, the peak amplitude of the bright component decreases slightly.

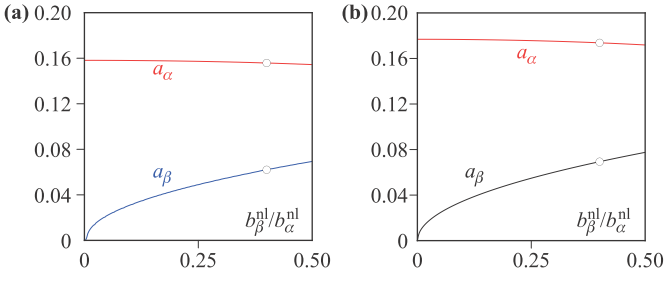

Fig. 3 **(a)** Peak amplitudes of the bright soliton component a_α and of the background of the dark component a_β of the vector edge soliton, as functions of $b_\beta^{\rm nl}/b_\alpha^{\rm nl}$ at $b_\alpha^{\rm nl} = 0.004$. **(b)** Same as (a) but for the bright-anti-bright vector edge soliton at $b_\alpha^{\rm nl} = 0.005$.

3.2 Propagation dynamics of valley Hall edge solitons

By superposing the envelopes onto the linear valley Hall edge states, as shown in Figs. 1(d) and (e), the scalar as well as the vector valley Hall edge solitons are established.

The propagation dynamics of the scalar bright valley Hall edge soliton is shown in Fig. 4, and that of the scalar dark valley Hall edge soliton is shown in Fig. 5. One finds that both the bright soliton and the dark soliton move

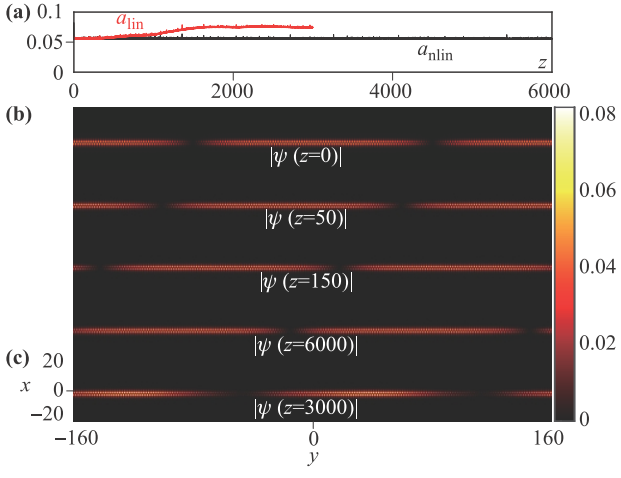

Fig. 5 Moving dark topological valley Hall edge soliton with $b^{\rm nl} = 0.0016$. Setup is as in Fig. 4.

along the negative y direction during propagation. After a long distance of $z = 6000$, the profile of the soliton does not change and the peak amplitude $a_{\rm nlin}$ does not reduce much [see the black curves in Fig. 4(a) and Fig. 5(a)]. For comparison, we also depict the linear propagation of the soliton input without including the nonlinearity in Eq. (1). During linear propagation, the bright soliton input spreads quickly and decays fast; the profile at $z = 1500$ is shown in Fig. 4(c). The peak amplitude $a_{\rm lin}$ of the soliton input during linear propagation is shown by the red curve in Fig. 4(a), and one can see that it reduces quickly. Similar phenomenon can be observed for the dark valley Hall edge soliton in linear propagation, as shown in Fig. 5(c). With the notches of the dark valley Hall edge soliton broadening, the background of the beam increases, as shown by the red curve in Fig. 5(a).

As mentioned before, the dispersion of the edge state in the lattice with type-II Dirac cones supports vector solitons because the second derivatives of the edge state can be either positive or negative, depending on the Bloch momentum. We choose two states as indicated by the blue and green dots in Fig. 1, with Bloch momenta being $k_y = -0.35K$ and $k_y = -0.16K$, respectively. The first-order derivatives of the two states are almost equal with the value of $b' \approx 0.42$. The second-order derivative of the blue state is $b'' \approx 0.86$ and that of the green state is $b'' \approx -0.53$. Superposing the envelopes in Fig. 2(c) onto the linear valley Hall edge states, one obtains the corresponding vector bright-dark valley Hall edge state.

The propagation of the bright-dark vector soliton is shown in Fig. 6. During nonlinear propagation, the vector soliton moves along the negative y direction with a constant speed, and its profile as well as its peak amplitude $\alpha_{\rm nlin}$ remain unchanged even after a long propagation distance [see the black curve in Fig. 6(a) and profiles at the selected distances in Fig. 6(b)]. Without self-action from the nonlinearity, the vector soliton input will lose its soliton property quickly. The corresponding peak amplitude $\alpha_{\rm lin}$ is indicated by the red curve in Fig. 6(a), and an exemplary profile of the vector soliton input at $z = 800$ during linear propagation is given in Fig. 6(c).

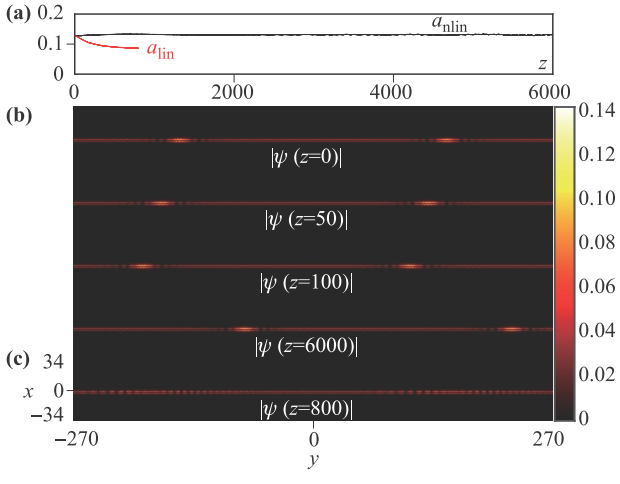

Fig. 6 Bright-dark vector topological valley Hall edge soliton with $b_\alpha^{\rm nl} = 0.004$ and $b_\beta^{\rm nl} = 0.0016$. Setup is as in Fig. 4.

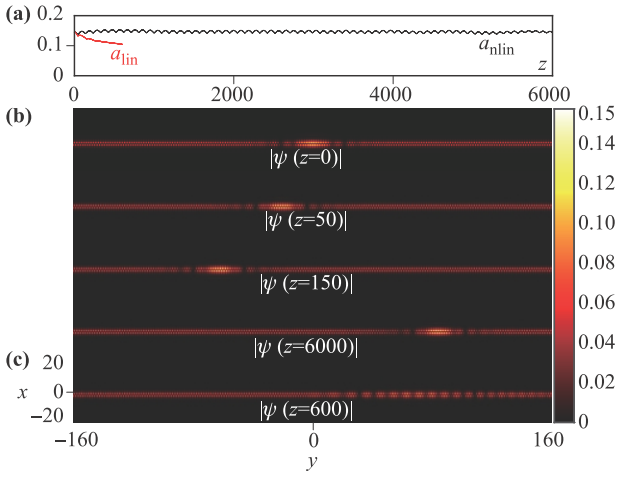

Fig. 7 Bright-anti-bright vector topological valley Hall edge soliton with $b_\alpha^{\rm nl} = 0.004$ and $b_\beta^{\rm nl} = 0.0016$. Setup is as in Fig. 4.

Finally, we turn to the propagation dynamics of the bright-anti-bright vector valley Hall edge soliton. The results are shown in Fig. 7. One finds that the propagation and phenomena connected with the bright-anti-bright valley Hall edge vector soliton are quite similar to the bright-dark vector soliton shown in Fig. 6. Therefore, the new bright-anti-bright vector valley Hall edge soliton is also demonstrated.

4 Conclusion

Summarizing, we have demonstrated the vector valley Hall edge solitons for the first time. These results are obtained in straight waveguide arrays that are arranged in the lattice landscape with innate type-II Dirac cones. We elaborately introduce refractive index detunings to lattice sites, in order to break the inversion symmetry of the lattice and establish a domain wall by combining two such lattices. On the domain walls, there appear valley Hall edge states. Superimposing soliton envelopes onto the linear valley Hall edge states, the scalar and vector valley Hall edge solitons are found, which include the bright-dark vector solitons and the new bright-anti-bright vector solitons. Since solitons have been reported in a variety of systems [73–75], we believe that our results can also be obtained in other systems in addition to the ordinary waveguide array.

Acknowledgements This work was supported by the National Natural Science Foundation of China (Nos. 12074308 and U1537210) and the Fundamental Research Funds for the Central Universities

(No. xzy012019038). Work in Qatar is supported by the NPRP-11S-1126-170033 project from the Qatar National Research Fund (a member of the Qatar Foundation).

References

1. M. Z. Hasan and C. L. Kane, Topological insulators, *Rev. Mod. Phys.* 82(4), 3045 (2010)
2. X. L. Qi and S. C. Zhang, Topological insulators and superconductors, *Rev. Mod. Phys.* 83(4), 1057 (2011)
3. R. Süsstrunk and S. D. Huber, Observation of phononic helical edge states in a mechanical topological insulator, *Science* 349(6243), 47 (2015)
4. S. D. Huber, Topological mechanics, *Nat. Phys.* 12(7), 621 (2016)
5. C. He, X. Ni, H. Ge, X. C. Sun, Y. B. Chen, M. H. Lu, X. P. Liu, and Y. F. Chen, Acoustic topological insulator and robust one-way sound transport, *Nat. Phys.* 12(12), 1124 (2016)
6. Y. G. Peng, C. Z. Qin, D. G. Zhao, Y. X. Shen, X. Y. Xu, M. Bao, H. Jia, and X. F. Zhu, Experimental demonstration of anomalous Floquet topological insulator for sound, *Nat. Commun.* 7(1), 13368 (2016)
7. A. V. Nalitov, D. D. Solnyshkov, and G. Malpuech, Polariton Z topological insulator, *Phys. Rev. Lett.* 114(11), 116401 (2015)
8. S. Klembt, T. H. Harder, O. A. Egorov, K. Winkler, R. Ge, M. A. Bandres, M. Emmerling, L. Worschech, T. C. H. Liew, M. Segev, C. Schneider, and S. Höfling, Exciton–polariton topological insulator, *Nature* 562(7728), 552 (2018)
9. G. Jotzu, M. Messer, R. Desbuquois, M. Lebrat, T. Uehlinger, D. Greif, and T. Esslinger, Experimental realization of the topological Haldane model with ultracold fermions, *Nature* 515(7526), 237 (2014)
10. N. Goldman, J. Dalibard, A. Dauphin, F. Gerbier, M. Lewenstein, P. Zoller, and I. B. Spielman, Direct imaging of topological edge states in cold-atom systems, *Proc. Natl. Acad. Sci. USA* 110(17), 6736 (2013)
11. F. D. M. Haldane and S. Raghu, Possible realization of directional optical waveguides in photonic crystals with broken time-reversal symmetry, *Phys. Rev. Lett.* 100(1), 013904 (2008)
12. Z. Wang, Y. Chong, J. D. Joannopoulos, and M. Soljacic, Observation of unidirectional backscattering-immune topological electromagnetic states, *Nature* 461(7265), 772 (2009)
13. M. Hafezi, E. A. Demler, M. D. Lukin, and J. M. Taylor, Robust optical delay lines with topological protection, *Nat. Phys.* 7(11), 907 (2011)
14. A. B. Khanikaev, S. Hossein Mousavi, W. K. Tse, M. Kargarian, A. H. MacDonald, and G. Shvets, Photonic topological insulators, *Nat. Mater.* 12(3), 233 (2013)
15. N. H. Lindner, G. Refael, and V. Galitski, Floquet topological insulator in semiconductor quantum wells, *Nat. Phys.* 7(6), 490 (2011)
16. M. C. Rechtsman, J. M. Zeuner, Y. Plotnik, Y. Lumer, D. Podolsky, F. Dreisow, S. Nolte, M. Segev, and A. Szameit, Photonic Floquet topological insulators, *Nature* 496(7444), 196 (2013)
17. L. J. Maczewsky, J. M. Zeuner, S. Nolte, and A. Szameit, Observation of photonic anomalous Floquet topological insulators, *Nat. Commun.* 8(1), 13756 (2017)
18. S. Mukherjee, A. Spracklen, M. Valiente, E. Andersson, P. Öhberg, N. Goldman, and R. R. Thomson, Experimental observation of anomalous topological edge modes in a slowly driven photonic lattice, *Nat. Commun.* 8(1), 13918 (2017)
19. L. Lu, J. D. Joannopoulos, and M. Soljačić, Topological photonics, *Nat. Photonics* 8(11), 821 (2014)
20. T. Ozawa, H. M. Price, A. Amo, N. Goldman, M. Hafezi, L. Lu, M. C. Rechtsman, D. Schuster, J. Simon, O. Zilberberg, and I. Carusotto, Topological photonics, *Rev. Mod. Phys.* 91(1), 015006 (2019)
21. M. Kim, Z. Jacob, and J. Rho, Recent advances in 2D, 3D and higher-order topological photonics, *Light Sci. Appl.* 9(1), 130 (2020)
22. M. Segev and M. A. Bandres, Topological photonics: Where do we go from here? *Nanophoton.* 10(1), 425 (2020)
23. H. F. Wang, B. Y. Xie, P. Zhan, M. H. Lu, and Y. F. Chen, Research progress of topological photonics, *Acta Phy. Sin.* 68(22), 224206 (2019) (in Chinese)
24. H. Wang, S. K. Gupta, B. Xie, and M. Lu, Topological photonic crystals: A review, *Front. Optoelectron.* 13(1), 50 (2020)
25. H. Liu, B. Xie, H. Cheng, J. Tian, and S. Chen, Topological photonic states in artificial microstructures, *Chin. Opt. Lett.* 19(5), 052602 (2021)
26. H. Liu, H. N. Wang, B. Y. Xie, H. Cheng, J. G. Tian, and S. Q. Chen, Progress of two-dimensional photonic topological insulators, *Chin. Opt.* 14(4), 935 (2021)
27. D. J. Bisharat, R. J. Davis, Y. Zhou, P. R. Bandaru, and D. F. Sievenpiper, Photonic topological insulators: A beginner's introduction, *IEEE Antennas Propag. Mag.* 63(3), 112 (2021)
28. D. Smirnova, D. Leykam, Y. Chong, and Y. Kivshar, Nonlinear topological photonics, *Appl. Phys. Rev.* 7(2), 021306 (2020)
29. Y. Ota, K. Takata, T. Ozawa, A. Amo, Z. Jia, B. Kante, M. Notomi, Y. Arakawa, and S. Iwamoto, Active topological photonics, *Nanophoton.* 9(3), 547 (2020)
30. M. Parto, Y. G. N. Liu, B. Bahari, M. Khajavikhan, and D. N. Christodoulides, Non-Hermitian and topological photonics: Optics at an exceptional point, *Nanophoton.* 10(1), 403 (2020)
31. B. Bahari, A. Ndao, F. Vallini, A. El Amili, Y. Fainman, and B. Kanté, Nonreciprocal lasing in topological cavities of arbitrary geometries, *Science* 358(6363), 636 (2017)
32. G. Harari, M. A. Bandres, Y. Lumer, M. C. Rechtsman, Y. D. Chong, M. Khajavikhan, D. N. Christodoulides, and M. Segev, Topological insulator laser: Theory, *Science* 359(6381), eaar4003 (2018)

33. M. A. Bandres, S. Wittek, G. Harari, M. Parto, J. Ren, M. Segev, D. N. Christodoulides, and M. Khajavikhan, Topological insulator laser: Experiments, *Science* 359(6381), eaar4005 (2018)
34. Y. V. Kartashov and D. V. Skryabin, Two-dimensional topological polariton laser, *Phys. Rev. Lett.* 122(8), 083902 (2019)
35. S. K. Ivanov, Y. Q. Zhang, Y. V. Kartashov, and D. V. Skryabin, Floquet topological insulator laser, *APL Photonics* 4(12), 126101 (2019)
36. Y. Zeng, U. Chattopadhyay, B. Zhu, B. Qiang, J. Li, Y. Jin, L. Li, A. G. Davies, E. H. Linfield, B. Zhang, Y. Chong, and Q. J. Wang, Electrically pumped topological laser with valley edge modes, *Nature* 578(7794), 246 (2020)
37. H. Zhong, Y. D. Li, D. H. Song, Y. V. Kartashov, Y. Q. Zhang, Y. P. Zhang, and Z. Chen, Topological valley Hall edge state lasing, *Laser Photonics Rev.* 14(7), 2000001 (2020)
38. Y. Gong, S. Wong, A. J. Bennett, D. L. Huffaker, and S. S. Oh, Topological insulator laser using valley-Hall photonic crystals, *ACS Photonics* 7(8), 2089 (2020)
39. D. Smirnova, A. Tripathi, S. Kruk, M. S. Hwang, H. R. Kim, H. G. Park, and Y. Kivshar, Room-temperature lasing from nanophotonic topological cavities, *Light Sci. Appl.* 9(1), 127 (2020)
40. W. Noh, H. Nasari, H. M. Kim, Q. Le-Van, Z. Jia, C. H. Huang, and B. Kanté, Experimental demonstration of single-mode topological valley-Hall lasing at telecommunication wavelength controlled by the degree of asymmetry, *Opt. Lett.* 45(15), 4108 (2020)
41. L. J. Maczewsky, M. Heinrich, M. Kremer, S. K. Ivanov, M. Ehrhardt, F. Martinez, Y. V. Kartashov, V. V. Konotop, L. Torner, D. Bauer, and A. Szameit, Nonlinearity-induced photonic topological insulator, *Science* 370(6517), 701 (2020)
42. Y. V. Kartashov and D. V. Skryabin, Bistable topological insulator with exciton-polaritons, *Phys. Rev. Lett.* 119(25), 253904 (2017)
43. W. Zhang, X. Chen, Y. V. Kartashov, D. V. Skryabin, and F. Ye, Finite-dimensional bistable topological insulators: From small to large, *Laser Photonics Rev.* 13(11), 1900198 (2019)
44. Y. Lumer, Y. Plotnik, M. C. Rechtsman, and M. Segev, Self-localized states in photonic topological insulators, *Phys. Rev. Lett.* 111(24), 243905 (2013)
45. S. Mukherjee and M. C. Rechtsman, Observation of Floquet solitons in a topological bandgap, *Science* 368(6493), 856 (2020)
46. M. J. Ablowitz, C. W. Curtis, and Y. P. Ma, Linear and nonlinear traveling edge waves in optical honeycomb lattices, *Phys. Rev. A* 90(2), 023813 (2014)
47. M. J. Ablowitz and J. T. Cole, Tight-binding methods for general longitudinally driven photonic lattices: Edge states and solitons, *Phys. Rev. A* 96(4), 043868 (2017)
48. M. J. Ablowitz and Y. P. Ma, Strong transmission and reflection of edge modes in bounded photonic graphene, *Opt. Lett.* 40(20), 4635 (2015)
49. D. Leykam and Y. D. Chong, Edge solitons in nonlinear photonic topological insulators, *Phys. Rev. Lett.* 117(14), 143901 (2016)
50. S. K. Ivanov, Y. V. Kartashov, L. J. Maczewsky, A. Szameit, and V. V. Konotop, Edge solitons in Lieb topological Floquet insulator, *Opt. Lett.* 45(6), 1459 (2020)
51. S. K. Ivanov, Y. V. Kartashov, L. J. Maczewsky, A. Szameit, and V. V. Konotop, Bragg solitons in topological Floquet insulators, *Opt. Lett.* 45(8), 2271 (2020)
52. S. K. Ivanov, Y. V. Kartashov, A. Szameit, L. Torner, and V. V. Konotop, Vector topological edge solitons in Floquet insulators, *ACS Photonics* 7(3), 735 (2020)
53. S. K. Ivanov, Y. V. Kartashov, M. Heinrich, A. Szameit, L. Torner, and V. V. Konotop, Topological dipole Floquet solitons, *Phys. Rev. A* 103(5), 053507 (2021)
54. S. K. Ivanov, Y. V. Kartashov, and V. V. Konotop, Four-wave mixing Floquet topological solitons, *Opt. Lett.* 46(19), 4710 (2021)
55. S. K. Ivanov, Y. V. Kartashov, and V. V. Konotop, Floquet defect solitons, *Opt. Lett.* 46(21), 5364 (2021)
56. Y. V. Kartashov and D. V. Skryabin, Modulational instability and solitary waves in polariton topological insulators, *Optica* 3(11), 1228 (2016)
57. D. R. Gulevich, D. Yudin, D. V. Skryabin, I. V. Iorsh, and I. A. Shelykh, Exploring nonlinear topological states of matter with exciton-polaritons: Edge solitons in kagome lattice, *Sci. Rep.* 7(1), 1780 (2017)
58. C. Li, F. Ye, X. Chen, Y. V. Kartashov, A. Ferrando, L. Torner, and D. V. Skryabin, Lieb polariton topological insulators, *Phys. Rev. B* 97(8), 081103 (2018)
59. Y. Q. Zhang, Y. V. Kartashov, and A. Ferrando, Interface states in polariton topological insulators, *Phys. Rev. A* 99(5), 053836 (2019)
60. D. A. Smirnova, L. A. Smirnov, D. Leykam, and Y. S. Kivshar, Topological edge states and gap solitons in the nonlinear Dirac model, *Laser Photonics Rev.* 13(12), 1900223 (2019)
61. W. Zhang, X. Chen, Y. V. Kartashov, V. V. Konotop, and F. Ye, Coupling of edge states and topological Bragg solitons, *Phys. Rev. Lett.* 123(25), 254103 (2019)
62. H. Zhong, S. Xia, Y. Zhang, Y. Li, D. Song, C. Liu, and Z. Chen, Nonlinear topological valley Hall edge states arising from type-II Dirac cones, *Adv. Photonics* 3(05), 056001 (2021)
63. Q. Tang, B. Ren, V. O. Kompanets, Y. V. Kartashov, Y. Li, and Y. Zhang, Valley Hall edge solitons in a photonic graphene, *Opt. Express* 29(24), 39755 (2021)
64. B. Ren, H. Wang, V. O. Kompanets, Y. V. Kartashov, Y. Li, and Y. Zhang, Dark topological valley Hall edge solitons, *Nanophoton.* 10(13), 3559 (2021)
65. Z. Y. Zhang, R. Wang, Y. Q. Zhang, Y. V. Kartashov, F. Li, H. Zhong, H. Guan, K. Gao, F. L. Li, Y. P. Zhang, and M. Xiao, Observation of edge solitons in photonic graphene, *Nat. Commun.* 11(1), 1902 (2020)
66. J. W. Liu, F. L. Shi, X. T. He, G. J. Tang, W. J. Chen, X. D. Chen, and J. W. Dong, Valley photonic crystals, *Adv. Phys. X* 6(1), 1905546 (2021)

67. K. C. Jin, H. Zhong, Y. D. Li, F. W. Ye, Y. P. Zhang, F. L. Li, C. L. Liu, and Y. Q. Zhang, Parametric type-II Dirac photonic lattices, *Adv. Quantum Technol.* 3(7), 2000015 (2020)

68. K. T. Wang, F. Xu, B. Wang, Y. Yu, and Y. Wei, Transport features of topological corner states in honeycomb lattice with multihollow structure, *Front. Phys. (Beijing)* 17(4), 43501 (2021)

69. S. Li, Z. M. Yu, Y. Yao, and S. A. Yang, Type-II topological metals, *Front. Phys. (Beijing)* 15(4), 43201 (2020)

70. S. Stützer, Y. Plotnik, Y. Lumer, P. Titum, N. H. Lindner, M. Segev, M. C. Rechtsman, and A. Szameit, Photonic topological Anderson insulators, *Nature* 560(7719), 461 (2018)

71. M. S. Kirsch, Y. Zhang, M. Kremer, L. J. Maczewsky, S. K. Ivanov, Y. V. Kartashov, L. Torner, D. Bauer, A. Szameit, and M. Heinrich, Nonlinear second-order photonic topological insulators, *Nat. Phys.* 17(9), 995 (2021)

72. D. Tan, Z. Wang, B. Xu, and J. Qiu, Photonic circuits written by femtosecond laser in glass: Improved fabrication and recent progress in photonic devices, *Adv. Photonics* 3(02), 024002 (2021)

73. Y. V. Kartashov, G. E. Astrakharchik, B. A. Malomed, and L. Torner, Frontiers in multidimensional self-trapping of nonlinear fields and matter, *Nat. Rev. Phys.* 1(3), 185 (2019)

74. B. A. Malomed and D. Mihalache, Nonlinear waves in optical and matter-wave media: A topical survey of recent theoretical and experimental results, *Rom. J. Phys.* 64, 106 (2019)

75. D. Mihalache, Localized structures in optical and matter-wave media: A selection of recent studies, *Rom. Rep. Phys.* 73, 403 (2021)